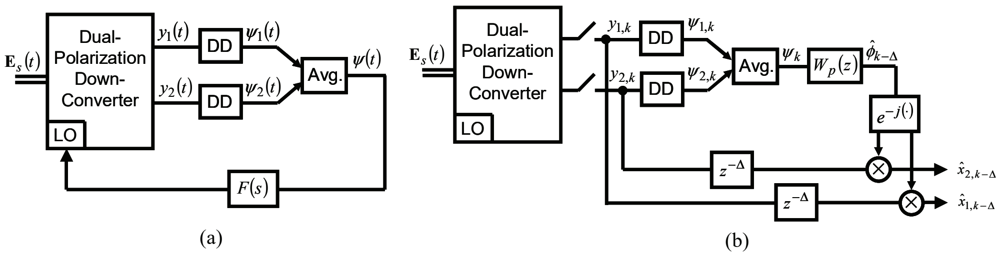

Fig. 18. Carrier synchronization for polarization-multiplexed systems, (a) PLL approach, (b) feedforward carrier synchronization approach.

5.4 Integration of receiver functions

A functional receiver needs to integrate carrier synchronization, linear equalization, nonlinear impairment compensation and symbol synchronization. If we consider NLPN to be the dominant nonlinear effect, and we assume IFWM is negligible, a hypothetical receiver structure is shown in Fig. 19. The sampled outputs of a dual-polarization downconverter are first passed through an NLPN compensator, which performs phase rotation proportional to the received amplitude. Linear equalization follows, yielding an output at one sample per symbol for which FF carrier synchronization is performed, followed by symbol decisions. The ordering of linear equalization before carrier synchronization is possible because from Table 8, we expect the laser linewidth $\Delta\nu$ to satisfy $\sim\Delta\nu T_s < 10^{-4}$. In contrast, the memory length of the linear equalizer is only 13 symbols for the worst case considered in Table 7. Since the carrier phase does not change significantly over the equalizer's memory, performance should not be compromised. The filter $W_p(z)$ in Fig. 19 exploits temporal correlation of laser phase noise and IFWM to mitigate both impairments. To make the system adaptive, we employ decision feedback to update equalizer coefficients, and the error signal is also passed through a timing error detector (TED) and loop filter to yield a control signal for the sampling clock. The design of the TED and loop filter for symbol synchronization can be found in [49].

A receiver structure with NLPN compensation first, followed by linear equalization and carrier synchronization has been employed in [72] and [73], and has been shown to reduce nonlinear phase variance for QPSK under certain transmission conditions. A receiver structure that can mitigate nonlinearities (including IFWM) for more general system designs is an ongoing research topic.

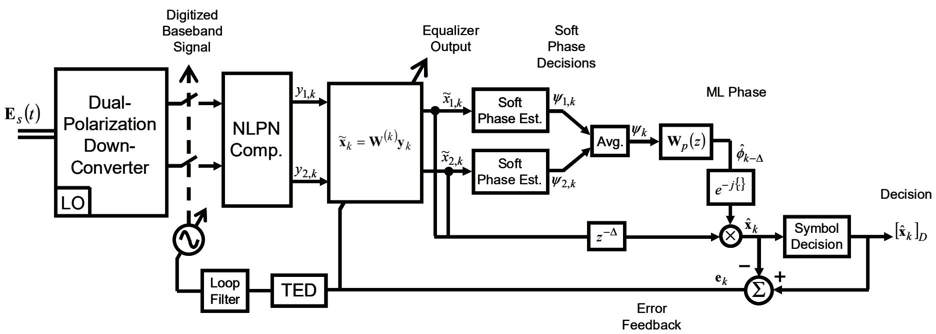

Fig. 19. Possible integration of nonlinear phase noise compensation, adaptive digital equalization and carrier synchronization.

#86543 - $15.00 USD Received 20 Aug 2007; revised 9 Nov 2007; accepted 12 Nov 2007; published 9 Jan 2008

6. Multi-carrier modulation: Orthogonal Frequency-Division Multiplexing

6.1 Introduction

Orthogonal frequency-division multiplexing (OFDM) is a multi-carrier technique that has been deployed in DSL and wireless systems [96,97], and is receiving increasing interest in optical fiber communications [98−101]. A multi-carrier system sends information over N_c frequency-division-multiplexed (FDM) channels, each modulated by a different carrier (Fig. 20(a)). For a given modulation format, with coherent detection, single-carrier and multi-carrier systems offer fundamentally the same spectral efficiency and power efficiency, but these may differ in practice, because of different impairments and implementation details. In OFDM, the modulation is implemented digitally by the inverse Fast Fourier Transform (IFFT) (Fig. 20(b)). We can write a multi-carrier signal as:

$$x_{ofdm}(t) = \sum_{m} \sum_{n=-N_c/2}^{N_c/2-1} x_{n,m} b\left(t - mT_{ofdm}\right) e^{j2\pi n f_d t} \,, \tag{55}$$

where $x_{n,m}$ denotes the m-th symbol transmitted on sub-carrier n, $b(t) = rect\left(t/T_{ofdm}\right)$ is the pulse shape, $T_{ofdm} = \left(N_c + N_{pre}\right)T_c$ is the OFDM symbol period, and $f_d = 1/\left(N_c T_c\right)$ is the frequency separation between sub-carriers. We define T_c as the chip period, and N_c and N_{pre} are integers. Suppose we sample Eq. (55) every chip period. We have:

$$x_{ofdm}(kT_c) = \sum_{m} \sum_{n=-N_c/2}^{N_c/2-1} x_{n,m} b\left(\left(k - m\left(N_c + N_{pre}\right)\right)T_c\right) e^{j\frac{2\pi nk}{N_c}} \,. \tag{56}$$

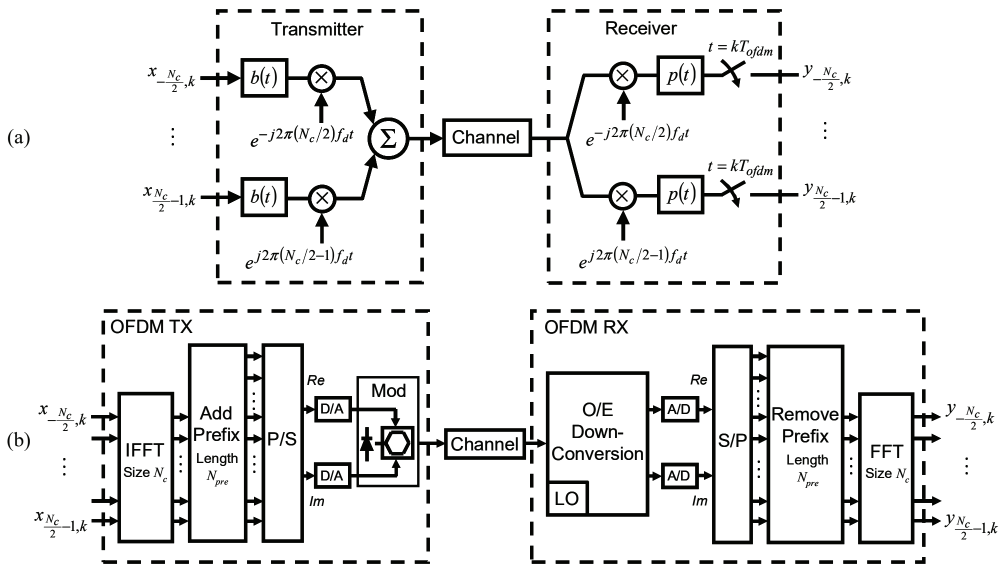

Fig. 20. Multi-carrier transmitter and receiver (a) analog implementation, (b) OFDM implementation.

#86543 - $15.00 USD Received 20 Aug 2007; revised 9 Nov 2007; accepted 12 Nov 2007; published 9 Jan 2008

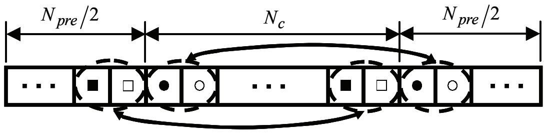

Fig. 21. OFDM symbol with cyclic prefix.

We note that the block of N_c samples $\left\{x_{ofdm}(kT_c):\ k_1\left(N_c+N_{pre}\right)-\frac{N_c}{2}\le k\le k_1\left(N_c+N_{pre}\right)+\frac{N_c}{2}-1\right\}$ is the IFFT of $\left\{x_{n,k_1}(kT_c):\ -\frac{N_c}{2}\le n\le\frac{N_c}{2}-1\right\}$ multiplied by a scaling factor. The remaining N_{pre} terms $\left\{x_{ofdm}(kT_c):\ k_1\left(N_c+N_{pre}\right)-\frac{N_c+N_{pre}}{2}\le k\le k_1\left(N_c+N_{pre}\right)+\frac{N_c+N_{pre}}{2}-1\right\}$ represent a periodic extension of the IFFT (Fig. 21), and are known as the *cyclic prefix*. The integers N_c and N_{pre} are thus the number of sub-carriers and the prefix length, respectively. We can generate Eq. (55) using the structure shown in Fig. 20(b). The inputs to the transmitter are the symbols modulating each sub-carrier, applied at a rate of $1/T_{ofdm}$. The IFFT and cyclic prefix computes the time-domain samples, and is followed by a parallel-to-serial (P/S) converter, digital-to-analog converter and Mach-Zehnder (MZ) modulator. The OFDM receiver performs the reverse operations. It can be shown that the receivers in Fig. 20(a) and (b) are equivalent when $p(t)=rect(t/N_cT_c)$.

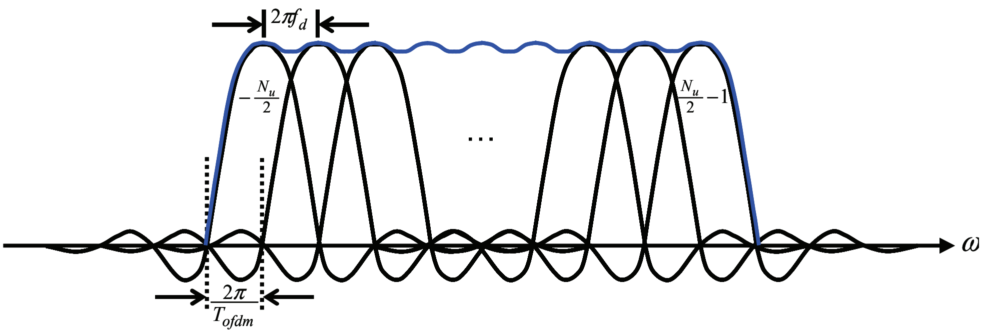

Fig. 22. Fourier transform of OFDM signal.

Assuming the transmitted symbols are independent: $E\left[x_{l,k}x_{n,m}^*\right]=0$ for $l\ne n$ or $k\ne m$, an OFDM signal has a spectrum of:

$$S_{xx}(\omega)=T_{ofdm}\sum_{n=-N_c/2}^{N_c/2}P_n\,\mathrm{sinc}^2\left(\frac{T_{ofdm}}{2\pi}(\omega-2\pi nf_d)\right), \tag{57}$$

where $P_n=E\left[\left|x_{n,m}\right|^2\right]$ is the average energy per symbol on sub-carrier *n*. A plot of Eq. (57) is shown in Fig. 22, where we assumed equal energy for all the sub-channels. The modulated sub-carriers are overlapping in frequency. The receiver is able to separate them by the Fast Fourier Transform (FFT) because $1/f_d$ is an integer multiple of the chip period T_c, i.e., the sub-carriers are "orthogonal" over the duration of an OFDM symbol.

#86543 - $15.00 USD Received 20 Aug 2007; revised 9 Nov 2007; accepted 12 Nov 2007; published 9 Jan 2008

In OFDM, oversampling can be implemented by not modulating the edge sub-carriers in Fig. 20. Supposing only N_u of the N_c sub-carriers are used, the effective oversampling rate is $\kappa_2 = N_c / N_u$. Compared to single-carrier transmission, oversampling can be easier to implement in OFDM, as it is possible to employ arbitrary ratios where a corresponding multi-rate solution for single-carrier modulation is prohibitively complex. Another advantage of OFDM is that the signal spectrum (Fig. 22) falls off more rapidly at the band edges than for a single-carrier signal. This is because the spectrum at each sub-carrier is $\mathrm{sinc}^2\left(\omega T_{ofdm}/2\pi\right)$, as opposed to $\mathrm{sinc}^2(\omega T_s/2\pi)$ for a single carrier. The $\left(N_c + N_{pre}\right)$-times steeper roll-off enables tighter optical filtering, and a lower oversampling rate.

6.2 Compensation of linear impairments and computational complexity

The cyclic prefix serves a special purpose in OFDM. Suppose we make N_{pre} large enough that $N_{pre}T_c$ is longer than the channel impulse response duration. The received OFDM symbol (after prefix removal) is a *circular convolution* between the transmitted OFDM symbol and the sampled impulse response of the channel. In the frequency domain, this corresponds to flat fading over each sub-channel, allowing a single-tap equalizer (complex multiplication) to compensate any amplitude and phase distortion at each sub-channel.

If the prefix length is insufficiently long, the circular convolution assumption no longer holds, and ISI and inter-carrier interference result [102]. It can be shown that the variance of ISI + ICI distortion at sub-carrier *k* is approximately [103]:

$$\sigma_{ISI+ICI}^2[k] \approx 2\sigma_x^2 \left(\sum_{m=0}^{\infty} \left| H_+\left[\tfrac{N_{pre}}{2} + m + 1; N; k\right] \right|^2 + \sum_{m=0}^{\infty} \left| H_-\left[\tfrac{N_{pre}}{2} + m + 1; N; k\right] \right|^2 \right), \tag{58}$$

where $H_+[s;N;k] = \sum_{n=0}^{N-1} h[s+n] e^{-j2\pi nk/N}$ and $H_-[s;N;k] = \sum_{n=0}^{N-1} h[-s-n] e^{-j2\pi(N-1-n)k/N}$ are *N*-point FFTs of the tails of the channel impulse response $h[n]$, which cause leakage of energy between OFDM symbols. $\sigma_x^2 = E\left[|x|^2\right]$ is the mean energy per sample in the time domain. Eq. (58) is exact when the transmitted signal samples $x[n]$ are i.i.d., which requires no oversampling, no cyclic prefix and equal power on all sub-channels. In practice, Eq. (58) is a good approximation when $\sum_{|n| > \frac{N_{pre}}{2} + N_c} |h[n]|^2$ is negligible and the oversampling rate is low.

Dual-polarization OFDM is implemented by operating two OFDM transmitters and receivers in parallel, as shown in Fig. 23 [104]. The single-tap equalizers become 2 × 2 matrices. In order to compensate PMD alone, the cyclic prefix must be longer than the PMD-induced delay spread (minus one chip). However, this is usually much shorter than the cyclic prefix required to compensate CD.

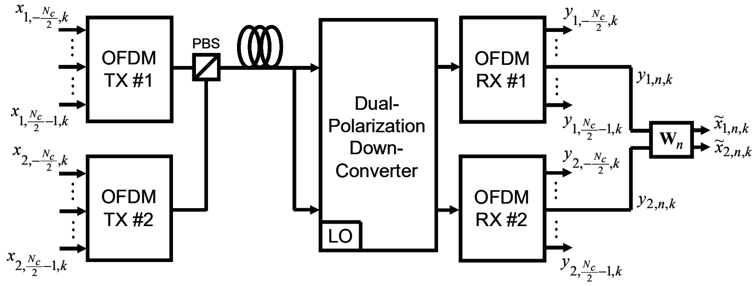

Fig. 23. Polarization-multiplexed OFDM transmitter and receiver with PMD compensation.

Table 9. OFDM parameters for 100 Gbit/s transmission using polarization-multiplexed 4-QAM. SMF (D = 17 ps/nm-km) with 2% under-compensation of CD is assumed. Target excess bandwidth factor of $\kappa_1 \leq 0.25$, oversampling ratio of $\kappa_2 \leq 1.25$, and impulse energy containment factor of $\kappa_3 \geq 0.98$ are assumed.

Transmission Distance (km)	Polarization-Multiplexed Transmission								
	4-QAM (4 bits/symbol)			8-QAM (6 bits/symbol)			16-QAM (8 bits/symbol)		
	N_{pre}	N_c	N_u	N_{pre}	N_c	N_u	N_{pre}	N_c	N_u
1,000	5	32	26	4	32	26	2	16	13
2,000	8	64	52	5	32	26	4	32	26
3,000	10	64	52	6	32	26	5	32	26
5,000	14	128	104	8	64	52	6	32	26

The number of sub-carriers required is determined by the channel's impulse response in conjunction with the target excess bandwidth factor (κ_1) and oversampling ratio (κ_2). Suppose a bit rate of R_b is required and all sub-carriers (with polarization multiplexing considered) encode b bits per symbol. The effective symbol rate is $R_s = R_b/b$, which gives an initial estimate of the chip rate as $1/T_c^{(1)} = R_s\left(1+\kappa_1^{(0)}\right)\kappa_2^{(0)}$, for which we can compute the impulse response $\mathbf{h}^{(i)}[n] \overset{\Delta}{=} \mathbf{h}\left(nT_c^{(i)}\right)$. Suppose we require a fraction κ_3 of the impulse energy be contained within the prefix:

$$\sum_{n=-N_{pre}^{(i)}/2}^{N_{pre}^{(i)}/2-1} \left|\mathbf{h}^{(i)}[n]\right|^2 \geq \kappa_3 \sum_{n=-\infty}^{\infty} \left|\mathbf{h}^{(i)}[n]\right|^2 . \tag{59}$$

Eq. (59) determines $N_{pre}^{(i)}$. To ensure the FFT size is an integer power of two, we set:

$$N_c^{(i)} = 2^{\left\lceil \log_2 N_{pre}^{(i)}/\kappa_1^{(0)} \right\rceil},\ N_u^{(i)} = \left\lfloor N_c^{(i)}/\kappa_2^{(0)} \right\rfloor, \tag{60}$$

where $\lceil\cdot\rceil$ denotes the nearest integer greater than or equal to. Eqs. (59) and (60) define new values of $\kappa_1^{(i)} = N_{pre}^{(i)}/N_c^{(i)}$ and $\kappa_2^{(i)} = N_c^{(i)}/N_u^{(i)}$ from which we can compute the new chip rate $1/T_c^{(i+1)} = R_s\left(1+\kappa_1^{(i)}\right)\kappa_2^{(i)}$. We iterate this process until stable parameter values are found. Table 9 shows the number of sub-carriers required to compensate CD for various propagation distances, assuming 100 Gbit/s polarization-multiplexed 4-QAM transmission through SMF with 2% CD under-compensation. As in the single-carrier case described in Section 5.1, CD dominates PMD in dictating system complexity. The complexity of OFDM is $R_s\kappa_2 \log_2 N_c$ complex multiplications per second at the transmitter and $R_s\left(\kappa_2 \log_2 N_c + 4\right)$ complex

#86543 - $15.00 USD Received 20 Aug 2007; revised 9 Nov 2007; accepted 12 Nov 2007; published 9 Jan 2008

multiplications at the receiver. It can be shown that the asymptotic complexity of OFDM grows as $R_s \log_2 R_s$, and is the same as single-carrier transmission. If adaptive equalization is required however, OFDM has a simpler update algorithm for the equalizer coefficients, as the filter taps and transmitted symbols are both in the frequency domain. In an FFT-based equalizer for single-carrier modulation, the filter taps are in the frequency domain, while the symbols are in the time domain. The update equation thus requires computing an FFT. In order to keep the overhead manageable, we expect the coefficient can only be updated infrequently for single-carrier.

6.3 Dynamic power allocation

For a frequency-selective channel, the optimum signal spectrum is given by water filling [105]. OFDM allows greater control of the signal spectrum as the power of each sub-carrier can be varied. In the limit of large N_u, the OFDM spectrum can approach continuous water filling. Sub-carriers transmitted at higher power can use denser constellations, such that similar BERs are obtained in all sub-carriers. OFDM with dynamic power allocation has been successfully employed in wireless systems to combat signal multi-path [106−108].

Frequency-selective channels are less fundamental to optical fiber than to wireless systems, because a fiber's main linear impairments, CD and PMD, are unitary transformations in a dual-polarization coherent receiver. In particular, PMD merely shifts energy from one polarization to another. Nevertheless, the ability to optimize power allocation may be useful when transmitting through cascaded optical elements, such as (de)interleavers, (de)multiplexers and ROADMs. In reconfigurable networks, OFDM would enable optimal power allocation across the sub-carriers based on instantaneous channel conditions.

6.4 Laser Phase Noise and Nonlinear Effects

Laser phase noise destroys the orthogonality of the sub-carriers and causes inter-channel interference (ICI), which has noise-like characteristics. Wu and Bar-Ness showed that the variance of ICI grows linearly with N_c [109]. Thus, the parameter that governs performance is the linewidth-to-sub-carrier-spacing ratio ($\Delta\nu T_c / N_c$). Phase noise considerations favor a smaller number of sub-carriers. At low phase noise, Armada and Calvo proposed using un-modulated pilot carriers to estimate the common phase error (CPE) for all the sub-channels [110]. At higher phase noise, the carrier phase can no longer be assumed as constant over an OFDM symbol. Wu and Bar-Ness found that using an MMSE equalizer that took into account both ICI and AWGN improves system performance [111]. However, this technique does not estimate or compensate for the phase noise process, unlike FF carrier synchronization for single-carrier modulation.

Carrier synchronization in OFDM may require an iterative algorithm. Suppose at the beginning of an OFDM symbol, an initial estimate of phase $\tilde{\phi}_k$ is known from the previous symbol. We can first de-rotate the entire OFDM symbol (N_c chips) by $\exp\left(-j\tilde{\phi}_k\right)$, and then perform the FFT, equalization and symbol detection. We can multiply the symbol decisions by the channel's frequency response and then take the IFFT to compute what the time samples should have been without phase noise. This allows the receiver to compute estimates $\psi_{k,m}$ of the carrier phase for each chip period. MMSE filtering can then be employed to find more reliable phase estimates $\hat{\phi}_{k,m}$ from $\psi_{k,m}$. We can de-rotate the OFDM symbol again, and a second iteration follows. This process can be repeated until convergence is achieved. The performance of such an algorithm has not been characterized.

OFDM is potentially susceptible to fiber nonlinearity due to its high peak-to-average power ratio (PAPR) [112]. Electrical pre- and post-compensation of nonlinearity for long-haul OFDM transmission has been studied in [113,114], while the effects of FWM have been investigated by [115].

#86543 - $15.00 USD Received 20 Aug 2007; revised 9 Nov 2007; accepted 12 Nov 2007; published 9 Jan 2008